Electronic Supplementary Material (ESI) for Catalysis Science & Technology.
This journal is © The Royal Society of Chemistry 2021

Supporting Information

Engineering the geometric and electronic structure of Ru via Ru-TiO_2 interaction for enhanced selective hydrogenation

Qiang Zhou‡, Zijiang Zhao‡, Zihao Yao‡, Zhongzhe Wei*, Songtao Huang, Fangjun Shao, Aiyuan Li, Jianguo Wang*

Institute of Industrial Catalysis, College of Chemical Engineering, State Key Laboratory Breeding Base of Green-Chemical Synthesis Technology, Zhejiang University of Technology, Hangzhou 310032 China.

Zhejiang Collaborative Innovation Center for High Value Utilization of Byproducts from Ethylene Project, Ningbo Polytechnic College, Ningbo 315800, Zhejiang, China.

SINOPEC Ningbo New Materials Research Institute Company Limited, Ningbo 315207, Zhejiang, China.

* Corresponding authors.

E-mail addresses: weizhzhe@zjut.edu.cn, jgw@zjut.edu.cn

‡ These authors contributed equally to this work.

Mass and Heat Transfer Calculations for selective hydrogenation of 6-chloroquinoline on Ru/TiO_2-Vo-250H.

The absence of mass transport resistances was checked by Weisz-Prater Criterion (CWP) for Internal Diffusion and Mears' Criterion (CM) for External Diffusion.

$$C_{WP} = \frac{r_{obs}\rho_c {R_p}^2}{D_{eff}C_s} < 1$$

$$C_M = \frac{r_{obs}\rho_c R_P n}{k_c C_{Ab}} < 0.15$$

Where r_{obs}: observed reaction rate, mol/kg_{cat}·s

n: reaction order

R_p: catalyst particle radius, m

ρ_c: bulk density of catalyst bed, kg/m^3

ρ_b: bulk density of catalyst bed, kg/m^3 = (1-Φ) ρ_c (Φ=porosity)

D_{eff}: effective diffusivity, m^2/s

C_s: gas concentration of A at the external surface of the catalyst, mol/m^3.

C_{Ab}: bulk gas concentration of A, mol/m^3.

k_c: external mass transfer coefficient, m/s

In the current work, a 50 mL autoclave was used as a batch reactor and the initial hydrogen pressure is 1.0 MPa. A catalyst particle size of $0.724*10^{-3}$ mm was employed for the kinetic study. For the Ru/TiO_2-Vo-250H catalyst, the obtained highest reaction rate was 2.67 mol $kg_{cat}^{-1}s^{-1}$

r_{obs}=2.67 mol/kgcat·s

n=1

R_p= 0.724*10^{-6} m

$\rho_c \approx \rho b \approx \rho cat$ = 6.255*10^2 kg/m^3

$C_s \approx C_{Ab}$= 384 mol/m^3

Calculation of effective diffusivity, D_{eff}

$$D_{eff} = 7.4 \times 10^{-10} \frac{(\varphi M_B)^{0.5} T}{\mu V_A^{0.6}}$$

Where φ: the association parameters of the solvent, 1.5

M_B: molar mass of solute, 163.6 g/mol

T: solvent temperature, 313 K

μ: viscosity of solvent, 0.82*10^{-2} P

V_A: the molecular volume of solute A at its normal boiling point, cm^3/mol, V_A=0.285 $V_c^{1.048}$, 128.7 cm^3/mol

V_c: the critical volume of solute A, cm^3/mol

$D_{eff} \approx$ 2.39*10^{-7} m^2/s

Calculation of external mass transfer coefficient, k_c

$$Sh = \frac{k_c d}{D_{AB}}$$

$$Sh = 0.6 Re^{0.5} Sc^{0.33}$$

$$U = \frac{d^2(\rho_s - \rho)g}{18\mu} = 5.29*10^{-8} \text{ m/s}$$

$$Re = \frac{U\rho d}{\mu} = 2.9945*10^{-8}$$

$$Sc = \frac{\mu}{\rho_s D} = 4.41$$

$Sh = 0.6 * (2.9945*10^{-8})^{0.5}(4.41)^{0.33} = 1.69*10^{-4}$

ρ: grain density, kg/m^3

μ: viscosity of the solute, P

d: catalyst particle diameter, m

U: free settling rate, m/s

ρ_s: the density of the solvent, kg/m^3

$k_c \approx 5.623*10^{-5}$ m/s

$$C_{WP} = \frac{r_{obs}\rho_c R_p^{\ 2}}{D_{eff}C_s} = [(2.67 \text{ mol/kgcat·s})*(6.255*10^2 \text{ kg/m}^3)*(0.724*10^{-6} \text{ m})^2] \ / \ [(2.39*10^{-7} \text{ m}^2/\text{s}) * (384 \text{ mol/m}^3)] = 9.53 * 10^{-6} < 1$$

$$C_M = \frac{r_{obs}\rho_c R_P n}{k_c C_{Ab}} = [(2.67 \text{ mol/kgcat·s}) * (6.255*10^2 \text{ kg/m}^3)*(0.724*10^{-6} \text{ m})*1] \ / \ [(5.623*10^{-5} \text{ m/s})*(384 \text{ mol/m}^3)] = 0.05 < 0.15$$

Therefore, internal and external diffusion effects could be neglected during the kinetic experiment.

Mears Criterion for External (Interphase) Heat Transfer

Calculation of heat transfer coefficient, h_t

$$\frac{h_t D}{\lambda} = Re^{\frac{2}{3}} Pr^{\frac{1}{3}} \left(\frac{u}{u_w}\right)^{-0.14}$$

$$Re = \frac{d^2 n \rho}{\mu}$$

$$Pr = \frac{C_\rho \mu}{\lambda}$$

d: stir magneton diameter, m

D: reactor diameter, m

n: revolving speed, r/min

ρ: solvent fluid density, kg/m^3

λ: solvent thermal conductivity, W/m·K

μ: viscosity of a solvent at body temperature, Pa·S

μ_w: viscosity of solvent at wall temperature, Pa·S

h_t: heat transfer coefficient, kj/s·m²·K

$$\left|\frac{-\Delta H(-r_{obs})\rho_c RE}{h_t T_b^2 R_g}\right| < 0.15$$

[(-205.32 kJ/mol)*(-2.67 mol/kgcat·s)*(6.255*10^2 kg/m^3)*(0.724*10^{-6} m)*(58.1 kJ/mol)] / [(524.5 kJ/s·m²·K)*(313^2 K^2)*(8.314*10^{-3} kJ/mol·K)] = 3.37*10^{-5} < 0.15

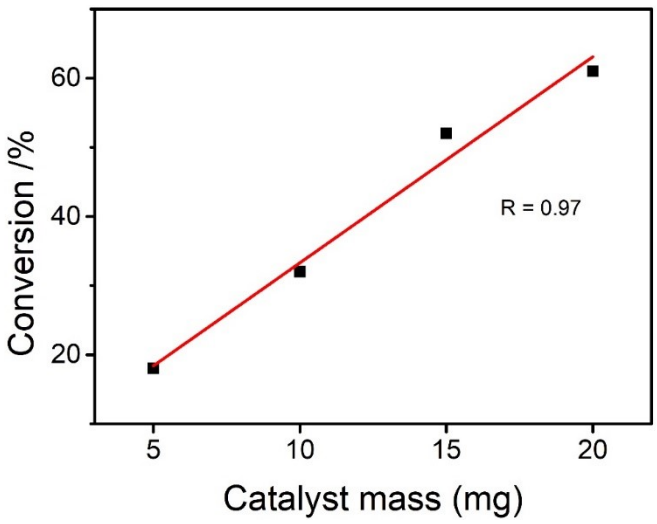

Fig. S1. The effect of catalyst mass on 6-chloroquinoline conversion. Reaction conditions: 6-chloroquinoline (0.2 mmol), catalyst (10 mg), ethanol (5 mL), 40 °C and 1 MPa H_2.

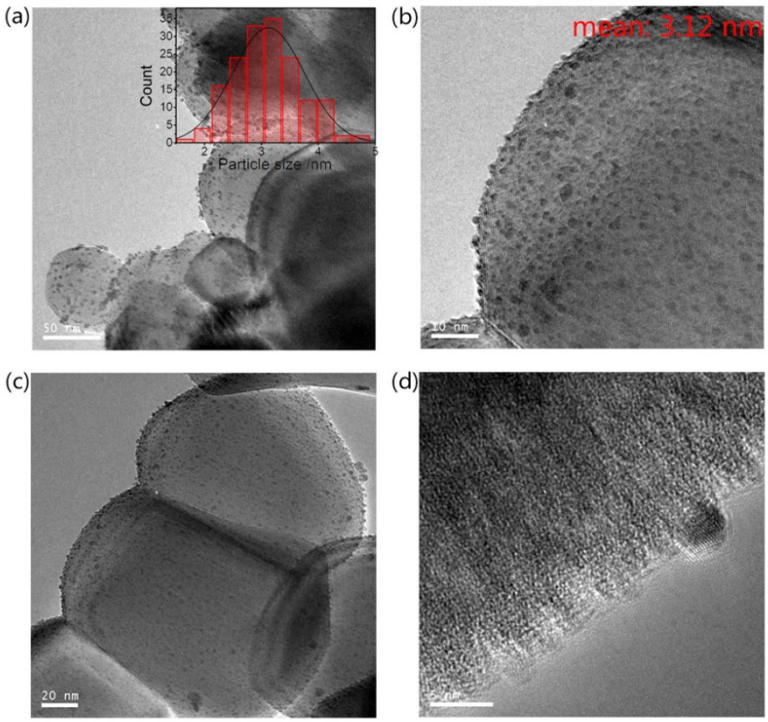

Fig. S2. Representative HRTEM images of Ru/P25-$NaBH_4$.

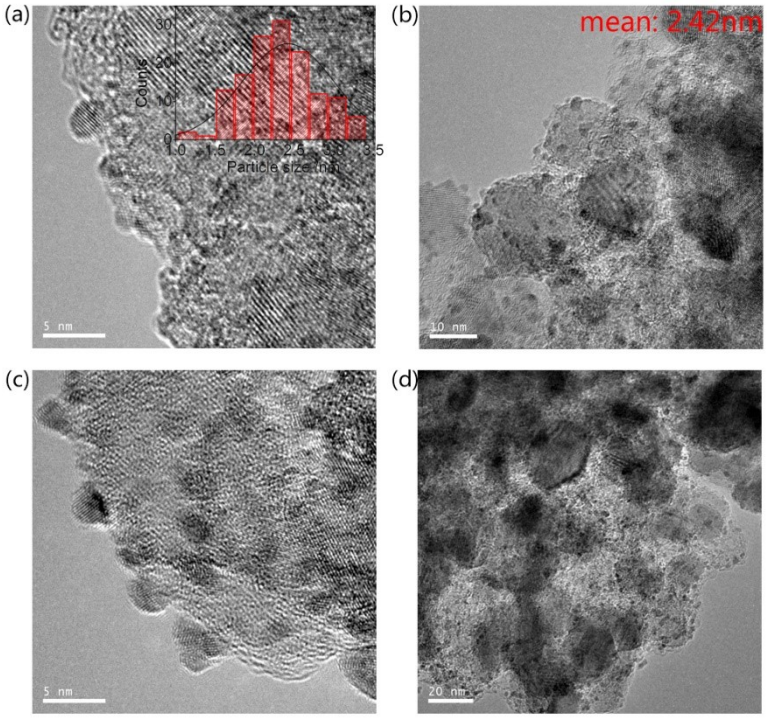

Fig. S3. Representative HRTEM images of Ru/TiO_2-Vo-$NaBH_4$.

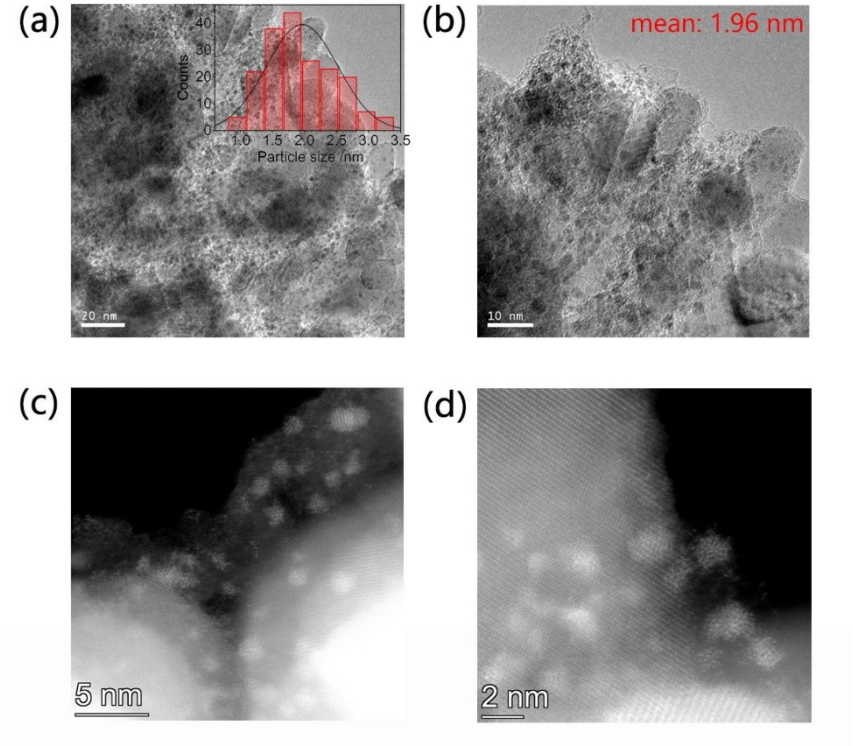

Fig. S4. (a, b) Representative HRTEM images of Ru/TiO_2-Vo-250H. (c, d) Representative HAADF-STEM images of Ru/TiO_2-Vo-250H.

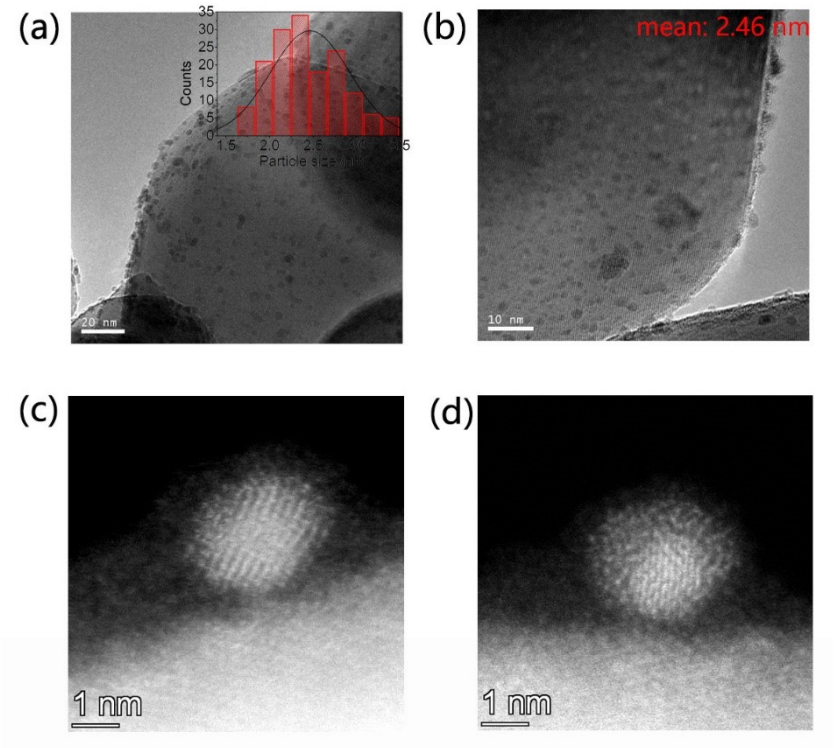

Fig. S5. (a, b) Representative HRTEM images of Ru/P25-250H. (c, d) Representative HAADF-STEM images of Ru/P25-250H.

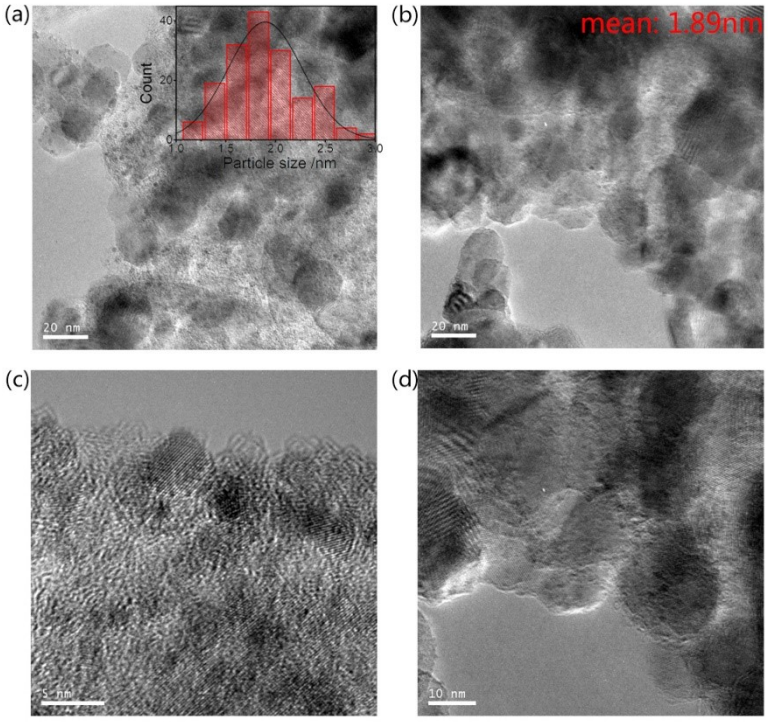

Fig. S6. Representative HRTEM images of Ru/TiO_2-Vo-150H.

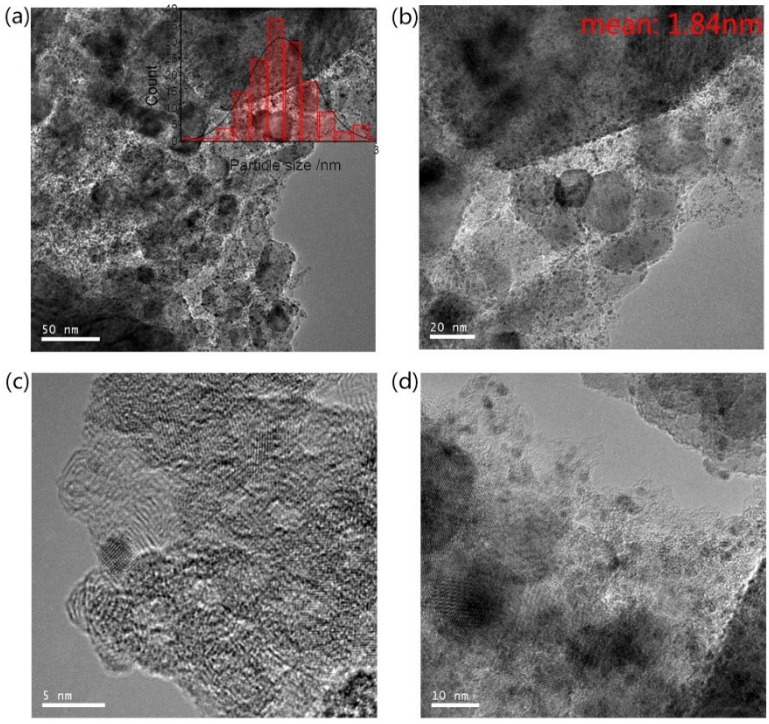

Fig. S7. Representative HRTEM images of Ru/TiO_2-Vo-350H.

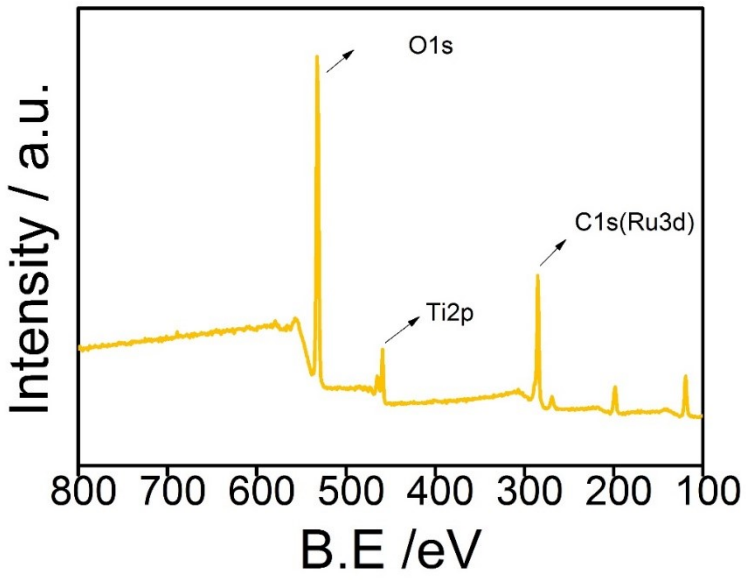

Fig. S8. XPS survey spectrum of Ru/TiO_2-Vo-250H.

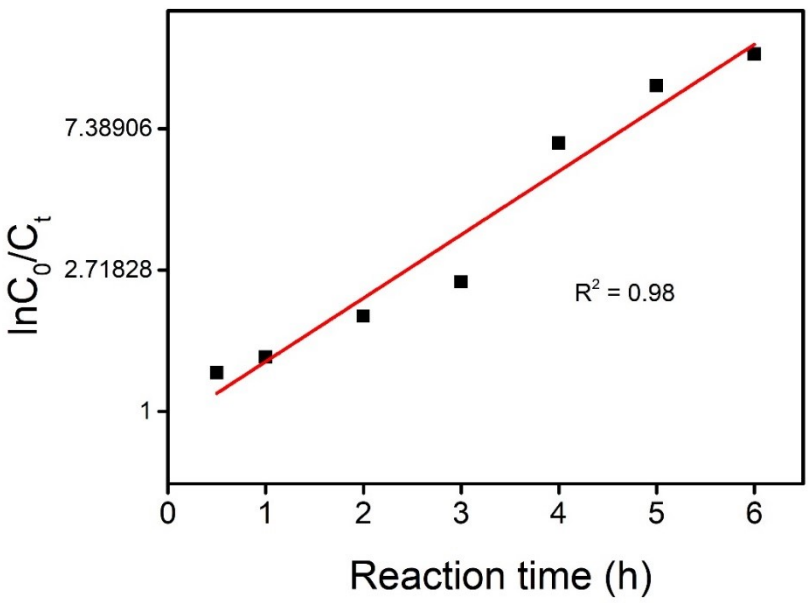

Fig. S9. ln C_0/C_t versus reaction time for the selective hydrogenation of 6-chloroquinoline over the Ru/TiO_2-Vo-250H catalyst at 40 °C, where C_0 represents the initial molar concentration of chloroquinoline and C_t represents the molar concentration of 6-chloroquinoline varied with reaction time. Reaction conditions: 6-chloroquinoline (0.2 mmol), catalyst (10 mg), ethanol (5 mL), 40 °C and 1 MPa H_2.

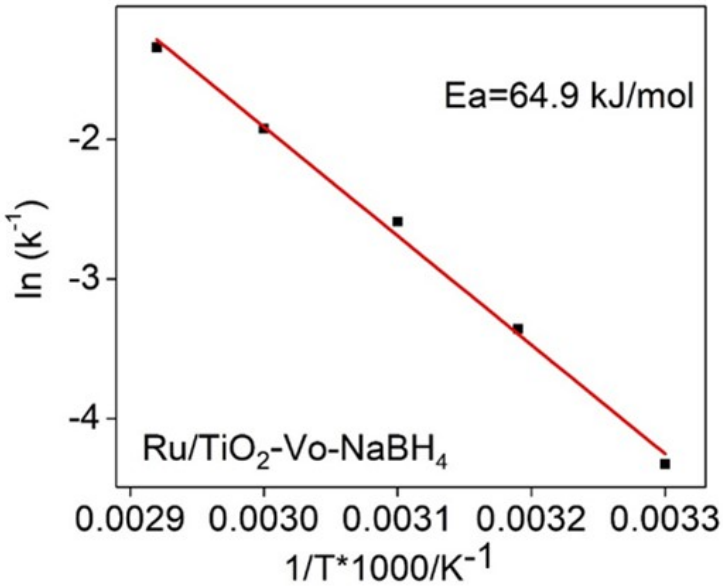

Fig. S10. Apparent activation energy (Ea) for the selective hydrogenation of 6-chloroquinoline over the Ru/TiO_2-Vo-$NaBH_4$.

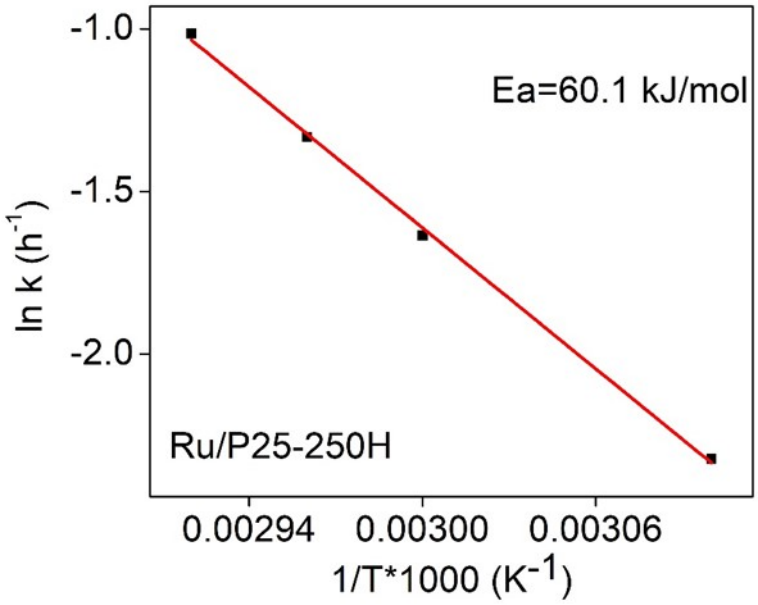

Fig. S11. Apparent activation energy (Ea) for the selective hydrogenation of 6-chloroquinoline over the Ru/P25-250H.

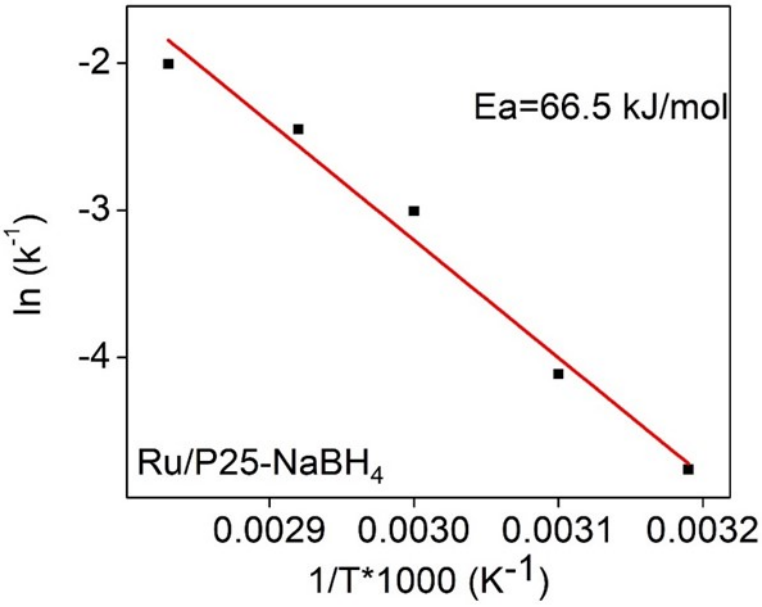

Fig. S12. Apparent activation energy (Ea) for the selective hydrogenation of 6-chloroquinoline over the Ru/P25-$NaBH_4$.

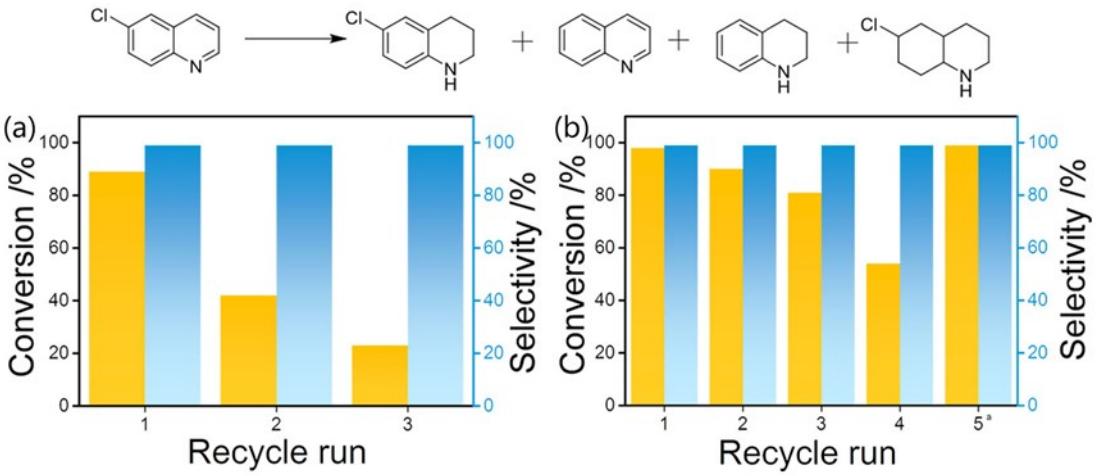

Fig. S13. (a) Catalytic stability for Ru/TiO_2-Vo-$NaBH_4$. (b) Catalytic stability for Ru/TiO_2-Vo-250H. The catalyst was treated with hydrogen after the fourth reaction.

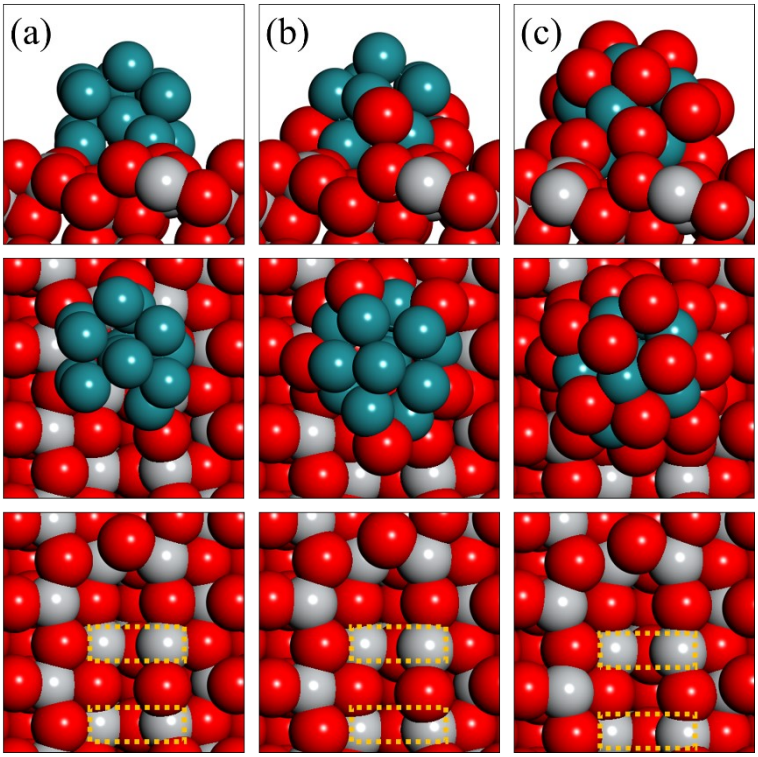

Fig. S14. (a) Structures of Ru/TiO_2-2Vo. (b) Structures of Ru/TiO_2-2Vo -half-O-Cover. (c) Structures of Ru/TiO_2-2Vo -total-O-Cover. The yellow dashed rectangles represent the oxygen vacancies.

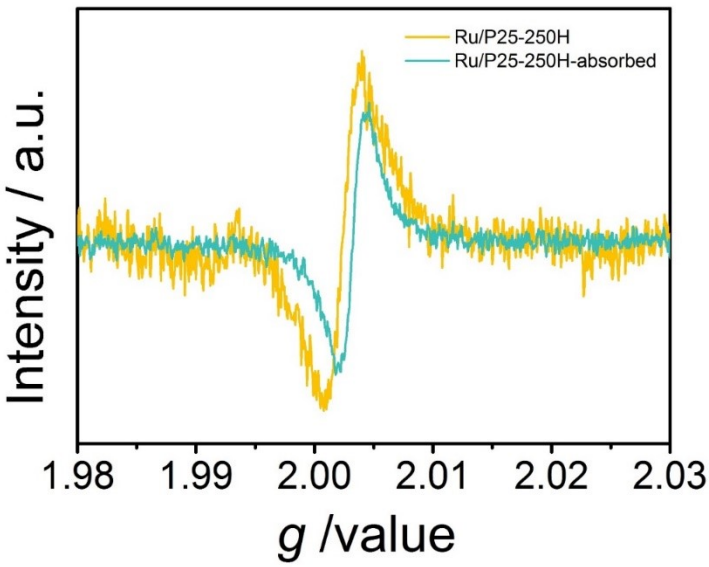

Fig. S15. EPR spectrum for Ru/P25-250H and Ru/P25-250H after adsorption of reactants.

Fig. S16. Physical mixed solution of Ru/TiO_2-Vo-250H and WO_3 before and after the reaction. Reaction conditions: 1.02 g mixture catalyst (Ru/TiO_2-Vo-250H : WO_3=1:50), 800 r/min, 5 mL solvent, 10 h, 1 MPa H_2.

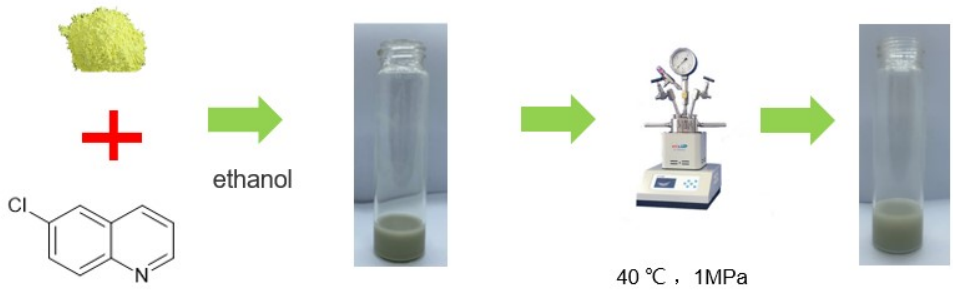

Fig. S17. Physical mixed solution of 6-chloroquinoline and WO_3 before and after the reaction. Reaction conditions: 1.033 g mixture catalyst (6-chloroquinoline : WO_3=1:30), 800 r/min, 5 mL solvent, 10 h, 1 MPa H_2.

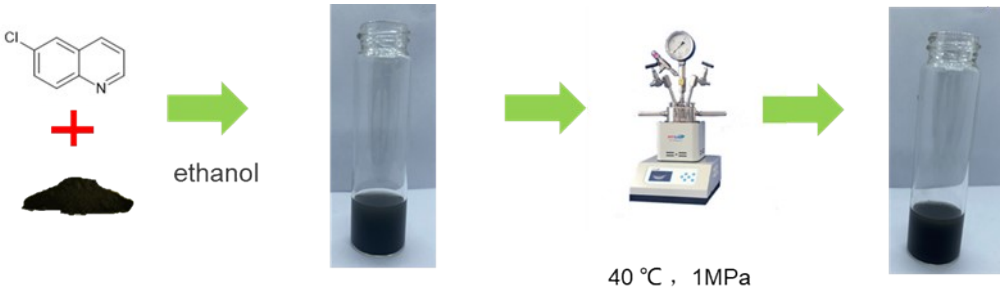

Fig. S18. Physical mixed solution of 6-chloroquinoline and Ru/TiO_2-Vo-250H before and after the reaction. Reaction conditions: 1.053 g mixture catalyst (Ru/TiO_2-Vo-250H : 6-chloroquinoline =33:20), 800 r/min, 5 mL solvent, 10 h, 1 MPa H_2.

Table S1 Conversion of 6-choroquinoline in different solvents.

Entry	Catalyst	Solvent	Conversion	Slectivity
1	Ru/TiO_2-Vo-250H	H_2O+ethanol	34	99
2	Ru/TiO_2-Vo-250H	DMF	11	99
3	Ru/TiO_2-Vo-250H	Tetrahydrofuran	0	99
4	Ru/TiO_2-Vo-250H	Para-xylene	8	99
5	Ru/TiO_2-Vo-250H	cyclohexane	4	99
6	Ru/TiO_2-Vo-250H	ethanol	72	99

Reaction conditions: 10 mg Catalyst, 0.25 mmol substrate 800 r/min, 5 mL solvent, 2 h, 1 MPa H_2.

Table S2 Summary of the recently reported literature about the apparent activation energy (Ea) of catalysts for hydrogenation of quinolines.

Catalyst	Reaction	Apparent activation energy (Ea) kJ/mol	Reference
BWT-Rh^{3+}	hydrogenation of quinoline	72	*J. Chem. Technol. Biotechnol.*, 2012, **87**, 1104-1110.
Ru/AC	hydrogenation of quinoline	63.44	*Microporous Mesoporous Mater.*, 2018, **256**, 10-17.
Ni/Al_2O_3	hydrogenation of quinoline	82±11	*Energy Fuels* 2020, **34**, 8769–8776
5% Ru/C	hydrogenation of quinoline	54.6	*Mol. Catal.*, 2018, **452**, 145-153.
Au@ SBA-15	hydrogenation of quinoline	58.7	*Nano Res.*, 2021, DOI: 10.1007/s12274-021-3732-1.
RhPt/ MCM-41	Hydrogenation of Aromatic Compounds	41.6	*J. Phys. Chem. C* 2021, **125**, 28, 15275–15282